# Genetic selection for small molecule production in competitive microfluidic droplets

Larry J. Millet[1,2], Jessica M. Velez[1,2], Joshua K. Michener[1, *]

(1) Biosciences Division, Oak Ridge National Laboratory, Oak Ridge, TN, 37830; (2) The Joint Research Activity Unit of The Bredesen Center for Interdisciplinary Research and Graduate Education, University of Tennessee, Knoxville, TN, 37996.

(*) Correspondence should be addressed to JKM (michenerjk@ornl.gov)

This manuscript has been authored by UT-Battelle, LLC under Contract No. DE-AC05-00OR22725 with the U.S. Department of Energy. The United States Government retains and the publisher, by accepting the article for publication, acknowledges that the United States Government retains a non-exclusive, paid-up, irrevocable, world-wide license to publish or reproduce the published form of this manuscript, or allow others to do so, for United States Government purposes. The Department of Energy will provide public access to these results of federally sponsored research in accordance with the DOE Public Access Plan (http://energy.gov/downloads/doe-public-access-plan).

**Abstract**

Biosensors can be used to screen or select for small molecule production in engineered microbes. However, mutations to the biosensor that interfere with accurate signal transduction are common, producing an excess of false positives. Strategies have been developed to avoid this limitation by physically separating the production pathway and biosensor, but these approaches have only been applied to screens, not selections. We have developed a novel biosensor-mediated selection strategy using competition between co-cultured bacteria. When applied to biosynthesis of *cis*,*cis*-muconate, we show that this strategy yields a selective advantage to producer strains that outweighs the costs of production. By encapsulating the competitive co-cultures into microfluidic droplets, we successfully enriched for muconate-producing strains from a large population of control non-producers. Facile selections for small molecule production will increase testing throughput for engineered microbes and allow for the rapid optimization of novel metabolic pathways.

33 ## Introduction

34 Engineered microbes can produce a range of valuable bioproducts, providing the basis for a
35 renewable bioeconomy[1]. However, initial strain construction efforts are often inefficient, and the
36 cost and effort required to optimize a proof-of-concept pathway can preclude further
37 development. New strategies for constructing libraries of mutant strains have accelerated the
38 design and build phases of the engineering cycle[2–4], but these efforts are limited by the
39 throughput of methods for identifying improved variants. Demonstrations of new library
40 construction methods frequently use phenotypes that can be linked to microbial growth or to
41 production of an easily-identifiable molecule, such as visibly-pigmented compounds. Using
42 similar approaches to engineer strains that produce higher concentrations of an arbitrary small
43 molecule is challenging.

44 One option for identifying rare variants from a mutant library is to include a biosensor, such
45 as a metabolite-responsive transcription factor or regulatory RNA, that reports on production of
46 the target small molecule[5,6]. These biosensors can be highly effective, but they also come with
47 several limitations. Most notably, the biosensor is typically expressed from the same cell that is
48 being engineered or evolved. As a result, mutations can occur in the sensor that disrupt the
49 desired regulation, producing false positive signals that require significant additional screening[6].
50 An intracellular biosensor also reports on the intracellular small molecule concentration. A
51 product that is rapidly exported may not show a differential signal as the production rate
52 changes. Similarly, a product that is rapidly imported may produce crosstalk between
53 neighboring cells. Finally, biosensors can be linked to selectable markers such as antibiotic
54 resistance genes or screenable markers such as fluorescent proteins. Selections typically enable
55 larger library sizes and require less infrastructure, but also amplify any concerns about false

56 positives during the selection.

57 Several strategies have been proposed to overcome these challenges using biosensors to
58 screen mutant libraries. Avoiding false positives requires separating the biosensor from the strain
59 being engineered in order to limit mutation accumulation in the biosensor. After the two
60 functions are separated, though, measurements of productivity then require either disruptive
61 methods to reintroduce the sensor into the producer strains[7] or some form of spatial structure to
62 prevent crosstalk between members of the library. Initial efforts often used colonies spread on
63 petri dishes, which limited the assay throughput[8]. More recent approaches rely on encapsulation
64 of cells inside microfluidic droplets[9–12]. By physically separating individual cells into distinct
65 droplets, interactions between cells can be eliminated. However, all of these approaches depend
66 on quantitative screens, limiting throughput and requiring fluorescence-activated cell sorters or
67 on-chip droplet sorters to isolate desired droplets. A biosensor-driven selection strategy would
68 simplify the process of isolating improved variants from a mutant library while expanding the
69 potential library size.

70 We have developed a selection strategy that uses competition between bacterial strains within
71 microfluidic droplets to select for small molecule biosynthesis. Production of the target small
72 molecule inhibits growth of a sensitive competitor and provides a selective advantage to the
73 producer (Figure 1A). We show that competitor strains can be rationally engineered to be
74 inhibited by a target small molecule, that production of the target provides an advantage to the
75 producer, and that spatial structure is required to prevent interactions between producer cells. By
76 combining these elements, we enriched true producer strains from a background of faster-
77 growing non-producers. These high-through selections for small molecule production will enable
78 rapid optimization of engineered microbes.

## Results and Discussion

### Strain design and construction

To establish a microbial competition mediated by small molecule production, two different strains are inoculated into microfluidic droplets. The producer strain synthesizes a target small molecule, while the competitor strain is inhibited by the synthesized target (Figure 1). We chose muconate as our target small molecule, with *Pseudomonas putida* as the producer strain and *Escherichia coli* as the competitor.

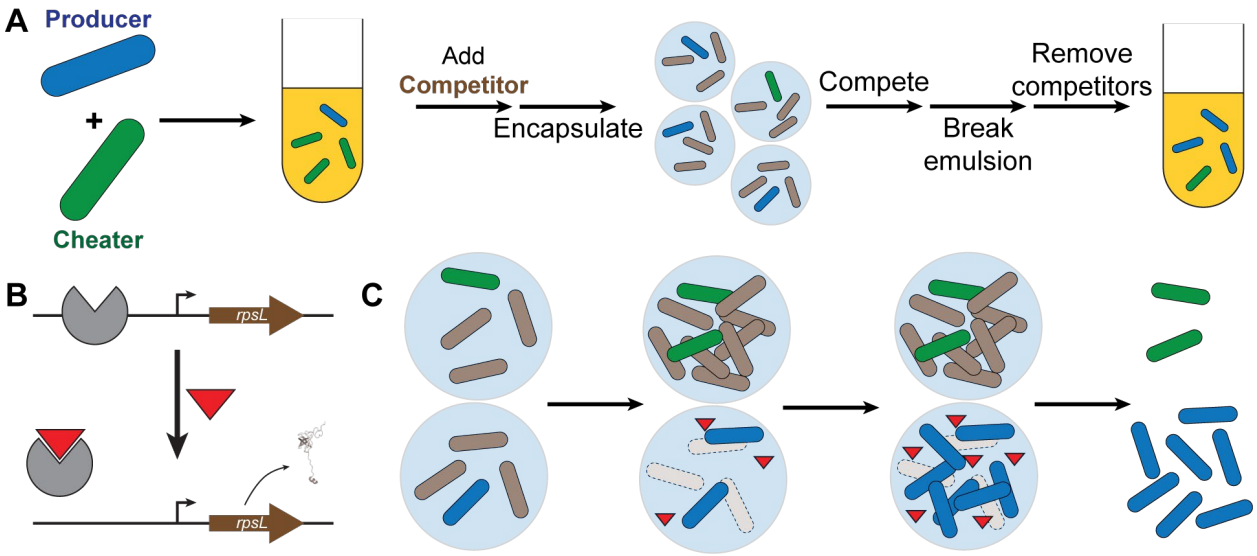


**Figure 1:** Competitive microfluidic droplets enable selections for small molecule production. (A) A simplified population contains a mix of producer strains (blue) that synthesize the desired small molecule and cheater strains (green) that do not. This population is then combined with the competitor strain (brown) and encapsulated into microfluidic droplets where the competitor is inhibited by the target molecule. The mixed cultures are grown to saturation, the emulsion is broken, and the producer cells increase in frequency due to the fitness benefit of eliminating the competitor strain. (B) The competitor strain is inhibited by the target molecule (red triangle) due

95 to regulation of the counterselectable marker *rpsL* by the biosensor. In the presence of the target
96 molecule, production of RpsL sensitizes the competitor strain to streptomycin. (C) In a droplet
97 containing a cheater, the competitor strain outcompetes the cheater and limits the yield.
98 Conversely, in a droplet containing a producer, production of the target molecule blocks
99 competitor growth and increases the yield of the producer strain.
100
101 The selection system consists of two strains, one engineered to produce muconate and the
102 other engineered to be inhibited by muconate. To build a suitable muconate-producing strain, we
103 started with *P. putida* CJ102, which was been previously engineered to synthesize muconate
104 from lignin-derived aromatic compounds[13]. The strain was further modified by deletion of the
105 adhesin *lapA*, to prevent biofilm formation[14]; deletion of a component of the type 6 secretion
106 system *tssA1*, to eliminate an alternative competitive factor[15]; deletion of the glucose
107 dehydrogenase *gcd*, prevent byproduct accumulation[16]; and introduction of a streptomycin-
108 resistance marker[17]. The resulting strain, JMP15, was then further modified by deletion of the
109 phenylpropanoid-CoA synthetase *fcs*[18] to produce a control strain, JMP26, that is incapable of
110 converting phenylpropanoids into muconate (Supplementary Figure 1A).
111 For the muconate-inhibited strain, we introduced a counterselection module into a
112 streptomycin-resistant strain of *E. coli*. The counterselection module consists of a constitutive
113 promoter driving expression of an operon containing a muconate transporter and a muconate-
114 responsive transcription factor, combined with a regulated promoter driving expression of a
115 counterselectable marker (Supplementary Figure 1B). We selected the *mucK* muconate
116 transporter from *Pseudomonas putida* and the muconate-responsive transcription factor *benM*
117 from *Acinetobacter baylyi*[19], and then expressed a streptomycin-sensitive allele of *rpsL* from the

118 BenM promoter. The counterselection module was synthesized *de novo* and cloned into pET-9a.
119 When the resulting plasmid was transformed into streptomycin-resistant *E. coli* REL606,
120 addition of muconate inhibited growth in a dose-dependent fashion, with growth completely
121 blocked at 10 mg/L muconate (Figure 2).

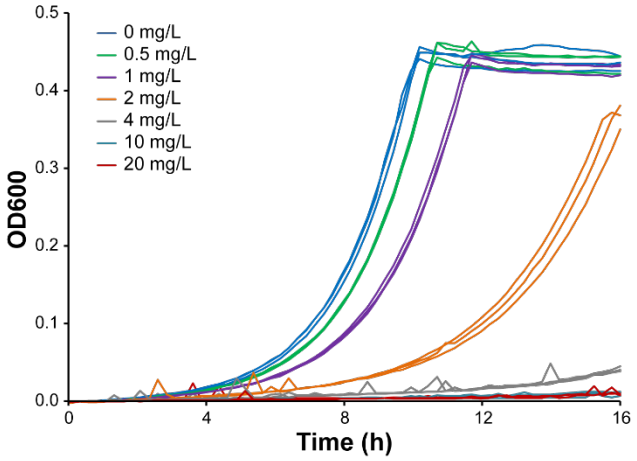


122

123 **Figure 2**: A muconate-responsive counterselection module demonstrates dose-dependent growth
124 inhibition. Streptomycin-resistant REL606 containing plasmid pJM242 was grown in minimal
125 medium containing ampicillin, streptomycin, and the indicated concentration of muconate. Three
126 biological replicates are shown.

127

128 **Muconate production is costly but provides a competitive advantage against sensitive *E.***
129 ***coli***

130 The engineered producer strain, JMP15, can convert coumarate to muconate in a series of
131 reactions that conserve little usable energy. Consequently, the strain grows more slowly in
132 minimal media containing glucose when coumarate is also added (Figure 3A). The control strain,
133 JMP26, does not show a growth difference.

134 We then grew the producer and control strains of *P. putida* in co-culture with the muconate-
135 sensitive *E. coli*. After growth, the *P. putida* concentration was measured by plating on selective

136 agar. When exogenous muconate was added, both *P. putida* strains showed large increases in
137 yield (Figure 3B). After addition of coumarate, the muconate-producing strain JMP15 showed a
138 small but significant fold increase in yield of 1.9±0.2 while the yield of the control strain was
139 unchanged. When grown in competition with a muconate-sensitive *E. coli*, muconate production
140 is costly to the cell, but the benefits of inhibiting *E. coli* growth offset the costs.

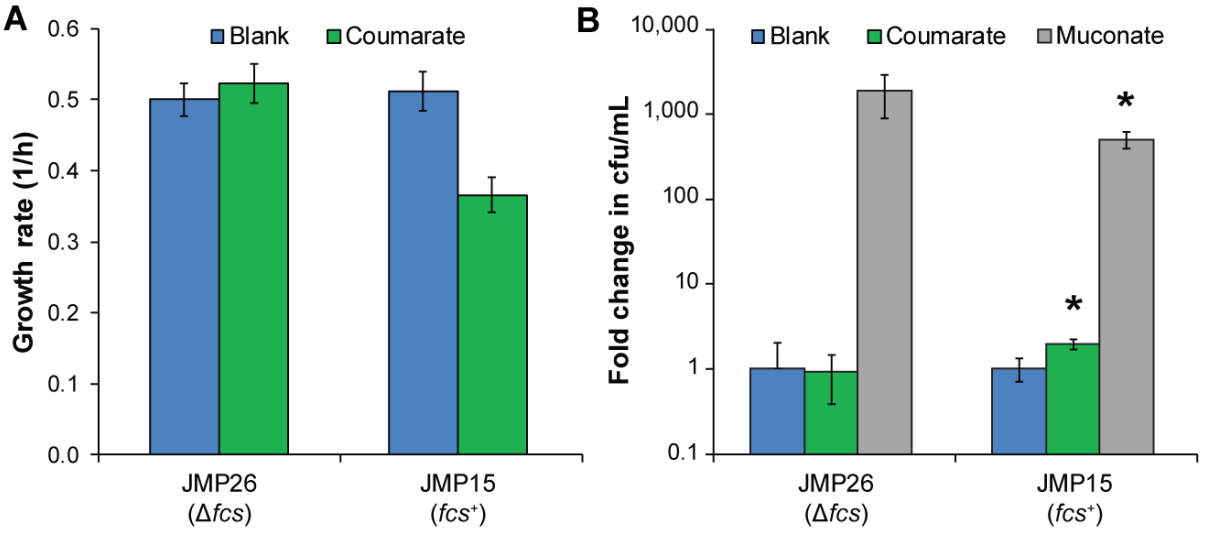


141

142 **Figure 3:** The benefits of muconate production outweigh the costs. (A) Addition of coumarate,
143 which can be converted into muconate, decreases the growth rate of JMP15. Deletion of the gene
144 encoding the first enzyme in coumarate metabolism, the CoA synthetase *fcs*, eliminates this
145 effect. (B) When grown in competition with *E. coli* that are sensitive to muconate, the addition of
146 coumarate provides a selective advantage only for the strain able to convert it into muconate. *: $p$
147 $< 0.05$, two-tailed t-test. Error bars show one standard deviation, calculated from three biological
148 replicates.

149

150 **Selection of muconate producers from mixed cultures requires spatial structure**

151 Muconate production provides an advantage when a pure culture of *P. putida* producers is
152 competed against *E. coli* (Figure 3B). However, when using a mixture of producer and control *P.*

153 *putida*, the costs are borne by the individual producers but the benefits, in terms of reduced *E.*
154 *coli* competition, are shared. Therefore, when a mixture of control and producer *P. putida* are
155 competed against *E. coli* in test tubes, we would expect the control strains to be more fit than the
156 producers. We tested this hypothesis by growing all three strains together, and then separating
157 out the *P. putida* and counting the fraction of JMP15 and JMP26 colonies. As predicted, the
158 population fraction of JMP15 was unchanged, averaging a 1.0-fold enrichment (Figure 4A).
159 Under these conditions, muconate production still increases the fitness of the *P. putida*, but the
160 control strains share equally in the benefits.

161 Successful selection for efficient producers, therefore, requires a method to limit the benefits
162 of muconate production to the producers. Microfluidic droplets can provide the necessary spatial
163 structure, by encapsulating each producer cell into a separate droplet. When a similar three-way
164 competition was conducted in droplets, the JMP15 population ratio increased significantly,
165 averaging a 6-fold increase from a single culture (Figure 4B and C).

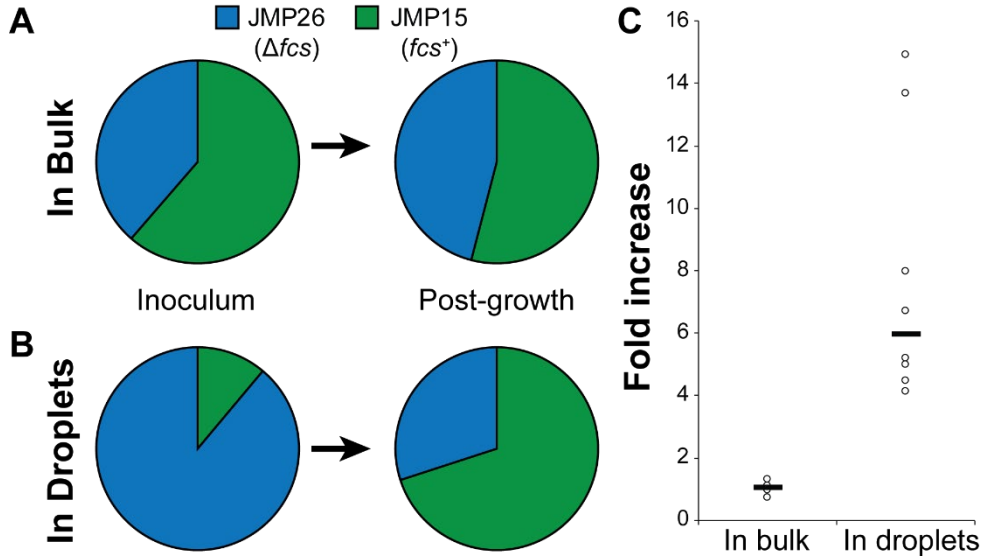

166

167 **Figure 4:** Spatial structure enables muconate selection. (A) A mixture of control and producer
168 strains were competed against muconate-sensitive *E. coli* in test tubes. The fraction of JMP15 in

169 the population did not change significantly. (B) When the mixed cultures were encapsulated into
170 microfluidic droplets, a single night of growth enriched for muconate producers. One
171 representative population ratio is shown for each condition. (C) The fold increase in JMP15
172 relative to JMP26 was calculated for each competition culture. Each point represents a single
173 biological replicate, and each set of competitions was repeated on at least two days. White
174 circles: individual cultures. Black bars: Distribution median.
175
176 This selection strategy has several key advantages. By separating the counterselection
177 module into a separate cell, mutations that prevent proper biosensor function yield false
178 negatives rather than false positives, by preventing producers from gaining the expected benefits
179 of muconate production. When selecting for rare phenotypes, false negatives are much more
180 easily tolerated than false positives. Similarly, the competitor strain can be eliminated and
181 reintroduced after every round of growth, preventing the accumulation of strains with mutated
182 biosensors.
183 This system also streamlines the process of using biosensors in diverse bacteria. The
184 producer and competitor strains can be entirely different species, individually chosen for specific
185 purposes. Rather than engineering the muconate biosensor into *P. putida*, we were able to leave
186 it in the more-tractable *E. coli* host. This muconate-sensitive competitor can then be used with
187 any muconate producing strain that has compatible culture conditions. The producer strain,
188 meanwhile, has no remnant of the biosensor that needs to be removed later. We also note that the
189 biosensor is not strictly necessary, as long as a competitor strain can be identified or engineered
190 that is inhibited by the product of interest. Finally, the validation of a new biosensor is
191 simplified. Frequently, biosensors are validated through exogenous addition of small molecules

192 and then used to sense compounds produced intracellularly. Here, the competitor strain is
193 intended to respond to exogenous products, so testing and application are performed under
194 equivalent conditions.

195 The selective pressures that result from this approach are complex. An increase in either
196 growth rate or muconate production would be expected to provide a selective advantage. In
197 general, we expect this complex selective pressure to be a benefit of this approach, since the
198 parallel selection for growth rate prevents the accumulation of mutations with strong fitness costs
199 and will yield robust strains. The selective pressure can also be tuned in multiple ways, including
200 modifying the sensitivity of the biosensor to its target, changing the initial population ratio of
201 producers and competitors, or engineering the competitor to grow more or less quickly.

202 While the initial selective advantage for a single round of growth in droplets was modest,
203 5.8 ± 1.5-fold, this represents a clear selection against nonproductive mutations. Mutant strains
204 with increased productivity will likely gain an additional selective advantage and produce a
205 larger fold enrichment.

206 New methods for strain and library construction have expanded the opportunities for large-
207 scale biological design. However, testing the resulting strains currently limits throughput. To
208 address this bottleneck, we have developed a flexible biosensor-driven selection strategy using
209 bacterial competition in microfluidic droplets. Using this approach, libraries generated through a
210 variety of methods can be rapidly tested to identify rare variants that improve productivity. By
211 increasing testing throughput, we can accelerate the development of new production strains and
212 shorten the time to market.

213

214 **Materials and Methods**

215 **Media and chemicals**

216 All chemicals were from Sigma-Aldrich unless otherwise noted. Strains were routinely
217 propagated in LB or M9 minimal medium containing 2 g/L glucose. Antibiotics were 50 µg/mL
218 kanamycin, 100 µg/mL ampicillin, and 50 µg/mL streptomycin. Stock solutions of muconate and
219 coumarate at 100 mg/mL were made fresh in DMSO and diluted to the appropriate
220 concentrations as needed. Microfluidic droplets used HFE-7500 (3M, St. Paul, MN) as the bulk
221 phase and 008-FluoroSurfactant (RAN Biotechnologies, Beverly, MA) as the surfactant.

222

223 **Genetic manipulation**

224 Strains JMP15 and JMP26 contain multiple mutations relative to the parental strain CJ102.
225 For gene deletions, the appropriate deletion construct, containing approximately 500 bp of
226 homology on both sides of the gene to be deleted, were synthesized *de novo* (IDT, Skokie, IL)
227 and assembled into pK18mobsacB[21] using the HiFi Assembly Master Mix (NEB, Ipswich, MA).
228 The resulting plasmids were transformed into *P. putida* by electroporation, followed by selection
229 on LB + kanamycin and counterselection on YT + 25% sucrose[22]. Gene deletions were verified
230 by colony PCR and Sanger sequencing (Eurofins Genomics, Louisville, KY). To introduce the
231 streptomycin resistance marker, plasmids pUX-BF13 and pBK-miniTn7-gfp3 were
232 cotransformed into the recipient *P. putida* strain by electroporation, followed by selection on LB
233 + kanamycin.

234

235 **Growth curves**

236 Strains for growth curve experiments were grown to saturation overnight at 30 °C in M9 + 2
237 g/L glucose + ampicillin. The cultures were then diluted 100-fold into fresh medium and grown

238 in 48-well plates in an Epoch 2 plate reader (BioTek, Winooski, VT) at 30 °C. Growth rates were
239 calculated using CurveFitter software[23].
240
241 **Bulk competition assays**
242 Strains JMP15, JMP26, and REL606+pJM242 were grown to saturation overnight at 30 °C
243 in M9 + 2 g/L glucose + ampicillin. The cultures were washed once and then diluted into 5 mL
244 of fresh M9 + 4 g/L glucose + ampicillin + streptomycin containing the relevant substrate as
245 indicated. Inoculation densities were OD 0.01 for JMP15 or JMP26, and 0.3 for
246 REL606+pJM242. For mixed *P. putida* cultures, the inoculation densities for JMP15 and JMP26
247 were 0.005, and the inoculum cultures were plated on LB + kanamycin as described below to
248 determine the initial population ratio. Cultures were grown overnight at 30 °C, then diluted and
249 plated on LB + kanamycin. For pure culture experiments, colonies were counted and adjusted for
250 the dilution factor. For mixed culture experiments, individual colonies were isolated and
251 genotyped by colony PCR of the *fcs* locus.
252
253 **Droplet competition assays**
254 Droplet competition assays were performed in a similar fashion as bulk assays. The *P.*
255 *putida* inoculation densities were decreased to 0.002 for pure cultures or 0.001 for each mixed
256 culture, to produce an average of one *P. putida* per 10 droplets. The *E. coli* inoculation density
257 was maintained at 0.15, yielding an average of approximately 6 *E. coli* per droplet. Initial
258 population ratios were determined by plating dilutions on LB + kanamycin agar.
259 Droplet encapsulation was performed on a Dolomite µEncapsulator system using a 50 µm
260 fluorophilic droplet chip, according to the manufacturer's directions. The *P. putida* and *E. coli*

261 cell suspensions were placed in separate channels of the reservoir immediately before
262 encapsulation. Flow rates of the driving fluids for *P. putida* and *E. coli* were set to 7 μL/min and
263 the surfactant-in-oil solution was held constant at 22 μL/min. Stability of the droplet generation
264 process was visually monitored to validate each run to completion. A typical run generated
265 approximately three million droplets with an average diameter of 60 μm. After one culture
266 reservoir was exhausted, the collection vial was removed, immediately capped, inspected for
267 quality (no visually distinguishable large droplets observed) and emulsion quantity (~500 μL
268 total, 200 μL emulsion layer), and incubated at 30 °C overnight.

269 After overnight growth, the emulsion was broken through the addition of 200 μL of
270 perfluorooctanol. The mixture was gently mixed by flicking the tube 5 times, then allowed to
271 settle for 5 min. The top aqueous layer (~120 μL) was removed into a new sterile microfuge
272 tube and serial dilutions ($10^{-1}$ to $10^{-3}$) plated onto LB + kanamycin agar. Following overnight
273 growth at 30 °C, densities were determined through colony counting, and population ratios by
274 colony PCR of the *fcs* locus as described above.

275

276 **Tables**

| Strain | Genotype | Source |
|---|---|---|
| REL606 | $F^-$ *tsx*467(Am) *araA*230 <u>*lon*</u> *rpsL*227($Sm^R$) *hsdR* | [24] |
| CJ102 | *P. putida* KT2440 Δ*catRBC*::Ptac:*catA* Δ*pcaHG*::Ptac:*aroY* | [25] |
| JMP9 | CJ102 Δ*lapA* | This work |
| JMP10 | CJ102 Δ*lapA* Δ*tssA1* | This work |
| JMP14 | CJ102 Δ*lapA* Δ*tssA1* Δ*gcd* | This work |
| JMP15 | CJ102 Δ*lapA* Δ*tssA1* Δ*gcd* $Km^R$ $Sm^R$ GFP | This work |
| JMP25 | CJ102 Δ*lapA* Δ*tssA1* Δ*gcd* Δ*fcs* | This work |
| JMP26 | CJ102 Δ*lapA* Δ*tssA1* Δ*gcd* Δ*fcs* $Km^R$ $Sm^R$ GFP | This work |

277 Table 1: Strains used in this work.

278

| Plasmid | Genotype | Source |
|---|---|---|
| pUX-BF13 | *mob*$^+$ Tn7 transposase Ap$^R$ | [17] |
| pBK-miniTn7-gfp3 | Km$^R$ Cm$^R$ Sm$^R$ Ap$^R$ *mob*$^+$ *gfp* | [17] |
| pJV1 | Km$^R$ *sacB mob*$^+$ Δ*tssA1* | This work |
| pJE364 | Km$^R$ *sacB mob*$^+$ Δ*lapA* | Unpublished |
| pJE365 | Km$^R$ *sacB mob*$^+$ Δ*gcd* | Unpublished |
| pJM242 | pBR322 Ap$^R$ apFab61-*mucK-benM* pbenM-*rpsL*$^*$ | This work |
| pJM384 | Km$^R$ *sacB mob*$^+$ Δ*fcs* | This work |

Table 2: Plasmids used in this work


## Acknowledgements

Gregg Beckham and Chris Johnson graciously provided strain CJ102. Strains pUX-BF13 and pBK-mini-Tn7-gfp3 were provided by Ole Nybroe. Plasmids pJE364 and pJE365 were provided by Joshua Elmore and Adam Guss. Oak Ridge National Laboratory is managed by UT-Battelle, LLC, for the DOE under Contract No. DE-AC05-00OR22725.

## Funding Information

This work was supported by the Laboratory Directed Research and Development program at the Oak Ridge National Laboratory.


## References


(1) Department of Energy, U. S. *2016 Billion-Ton Report: Advancing Domestic Resources for a Thriving Bioeconomy, Volume 1: Economic Availability of Feedstocks.*; Langholtz, M. H., Stokes, B. J., Eaton, L. M., Eds.; Oak Ridge, TN, 2016.

(2) Garst, A. D.; Bassalo, M. C.; Pines, G.; Lynch, S. A.; Halweg-Edwards, A. L.; Liu, R.; Liang, L.; Wang, Z.; Zeitoun, R.; Alexander, W. G.; et al. Genome-Wide Mapping of Mutations at Single-Nucleotide Resolution for Protein, Metabolic and Genome

297 Engineering. *Nat. Biotechnol.* **2016**, *35* (1), 48–55.

298 (3) Halperin, S. O.; Tou, C. J.; Wong, E. B.; Modavi, C.; Schaffer, D. V.; Dueber, J. E.
299 CRISPR-Guided DNA Polymerases Enable Diversification of All Nucleotides in a
300 Tunable Window. *Nature* **2018**, *560* (7717), 248–252.

301 (4) Wang, H. H.; Isaacs, F. J.; Carr, P. A.; Sun, Z. Z.; Xu, G.; Forest, C. R.; Church, G. M.
302 Programming Cells by Multiplex Genome Engineering and Accelerated Evolution. *Nature*
303 **2009**, *460* (7257), 894–898.

304 (5) Tang, S.-Y.; Cirino, P. C. Design and Application of a Mevalonate-Responsive
305 Regulatory Protein. *Angew. Chemie Int. Ed.* **2011**, *50* (5), 1084–1086.

306 (6) Michener, J. K.; Smolke, C. D. High-Throughput Enzyme Evolution in Saccharomyces
307 Cerevisiae Using a Synthetic RNA Switch. *Metab. Eng.* **2012**, *14* (4), 306–316.

308 (7) Esvelt, K. M.; Carlson, J. C.; Liu, D. R. A System for the Continuous Directed Evolution
309 of Biomolecules. *Nature* **2011**, *472* (7344), 499–503.

310 (8) Pfleger, B. F.; Pitera, D. J.; Newman, J. D.; Martin, V. J. J.; Keasling, J. D. Microbial
311 Sensors for Small Molecules: Development of a Mevalonate Biosensor. *Metab. Eng.*
312 **2007**, *9* (1), 30–38.

313 (9) Agresti, J. J.; Antipov, E.; Abate, A. R.; Ahn, K.; Rowat, A. C.; Baret, J.-C.; Marquez, M.;
314 Klibanov, A. M.; Griffiths, A. D.; Weitz, D. A. Ultrahigh-Throughput Screening in Drop-
315 Based Microfluidics for Directed Evolution. *Proc. Natl. Acad. Sci. U. S. A.* **2010**, *107* (9),
316 4004–4009.

317 (10) Wang, B. L.; Ghaderi, A.; Zhou, H.; Agresti, J.; Weitz, D. A.; Fink, G. R.;
318 Stephanopoulos, G. Microfluidic High-Throughput Culturing of Single Cells for Selection
319 Based on Extracellular Metabolite Production or Consumption. *Nat. Biotechnol.* **2014**, *32*

320 (5), 473–478.

321 (11) Siedler, S.; Khatri, N. K.; Zsohár, A.; Kjærbølling, I.; Vogt, M.; Hammar, P.; Nielsen, C.
322 F.; Marienhagen, J.; Sommer, M. O. A. O. A.; Joensson, H. N. Development of a Bacterial
323 Biosensor for Rapid Screening of Yeast *p* -Coumaric Acid Production. *ACS Synth. Biol.*
324 **2017**, acssynbio.7b00009.

325 (12) Abatemarco, J.; Sarhan, M. F.; Wagner, J. M.; Lin, J.-L.; Liu, L.; Hassouneh, W.; Yuan,
326 S.-F.; Alper, H. S.; Abate, A. R. RNA-Aptamers-in-Droplets (RAPID) High-Throughput
327 Screening for Secretory Phenotypes. *Nat. Commun.* **2017**, *8* (1), 332.

328 (13) Vardon, D. R.; Rorrer, N. A.; Salvachúa, D.; Settle, A. E.; Johnson, C. W.; Menart, M. J.;
329 Cleveland, N. S.; Ciesielski, P. N.; Steirer, K. X.; Dorgan, J. R.; et al. Cis,Cis-Muconic
330 Acid: Separation and Catalysis to Bio-Adipic Acid for Nylon-6,6 Polymerization. *Green*
331 *Chem.* **2016**, *18* (11), 3397–3413.

332 (14) Espinosa-Urgel, M.; Salido, A.; Ramos, J. L. Genetic Analysis of Functions Involved in
333 Adhesion of Pseudomonas Putida to Seeds. *J. Bacteriol.* **2000**, *182* (9), 2363–2369.

334 (15) Bernal, P.; Allsopp, L. P.; Filloux, A.; Llamas, M. A. The Pseudomonas Putida T6SS Is a
335 Plant Warden against Phytopathogens. *ISME J.* **2017**, *11* (4), 972–987.

336 (16) del Castillo, T.; Ramos, J. L.; Rodríguez-Herva, J. J.; Fuhrer, T.; Sauer, U.; Duque, E.
337 Convergent Peripheral Pathways Catalyze Initial Glucose Catabolism in Pseudomonas
338 Putida: Genomic and Flux Analysis. *J. Bacteriol.* **2007**, *189* (14), 5142–5152.

339 (17) Koch, B.; Jensen, L. E.; Nybroe, O. A Panel of Tn7-Based Vectors for Insertion of the
340 Gfp Marker Gene or for Delivery of Cloned DNA into Gram-Negative Bacteria at a
341 Neutral Chromosomal Site. *J. Microbiol. Methods* **2001**, *45* (3), 187–195.

342 (18) Nelson, K. E.; Weinel, C.; Paulsen, I. T.; Dodson, R. J.; Hilbert, H.; Martins dos Santos,

343 V. A. P.; Fouts, D. E.; Gill, S. R.; Pop, M.; Holmes, M.; et al. Complete Genome
344 Sequence and Comparative Analysis of the Metabolically Versatile Pseudomonas Putida
345 KT2440. *Environ. Microbiol.* **2002**, *4* (12), 799–808.
346 (19) Rogers, J. K.; Church, G. M. Genetically Encoded Sensors Enable Real-Time Observation
347 of Metabolite Production. *Proc. Natl. Acad. Sci. U. S. A.* **2016**, *113* (9), 2388–2393.
348 (20) Bachmann, H.; Fischlechner, M.; Rabbers, I.; Barfa, N.; Branco dos Santos, F.; Molenaar,
349 D.; Teusink, B. Availability of Public Goods Shapes the Evolution of Competing
350 Metabolic Strategies. *Proc. Natl. Acad. Sci. U. S. A.* **2013**, *110* (35), 14302–14307.
351 (21) Schäfer, A.; Tauch, A.; Jäger, W.; Kalinowski, J.; Thierbach, G.; Pühler, A. Small
352 Mobilizable Multi-Purpose Cloning Vectors Derived from the Escherichia Coli Plasmids
353 PK18 and PK19: Selection of Defined Deletions in the Chromosome of Corynebacterium
354 Glutamicum. *Gene* **1994**, *145* (1), 69–73.
355 (22) Johnson, C. W.; Beckham, G. T. Aromatic Catabolic Pathway Selection for Optimal
356 Production of Pyruvate and Lactate from Lignin. *Metab. Eng.* **2015**, *28*, 240–247.
357 (23) Delaney, N. F.; Kaczmarek, M. E.; Ward, L. M.; Swanson, P. K.; Lee, M.-C.; Marx, C. J.
358 Development of an Optimized Medium, Strain and High-Throughput Culturing Methods
359 for Methylobacterium Extorquens. *PLoS One* **2013**, *8* (4), e62957.
360 (24) Sniegowski, P. D.; Gerrish, P. J.; Lenski, R. E. Evolution of High Mutation Rates in
361 Experimental Populations of E. Coli. *Nature* **1997**, *387* (6634), 703–705.
362 (25) Johnson, C. W.; Salvachúa, D.; Khanna, P.; Smith, H.; Peterson, D. J.; Beckham, G. T.
363 Enhancing Muconic Acid Production from Glucose and Lignin-Derived Aromatic
364 Compounds via Increased Protocatechuate Decarboxylase Activity. *Metab. Eng. Commun.*
365 **2016**, *3*, 111–119.